JOURNAL OF MATERIALS SCIENCE 22 (1987) 363–373

Microstructure and phase transformations in duplex 316 manual metal arc weld metals: the role of carbon

R. A. FARRAR
Department of Mechanical Engineering, The University of Southampton, Hampshire, UK

The nature and kinetics of the phase transformation of metastable δ-ferrite in two duplex stainless steel manual metal arc weld metals has been studied at two carbon levels. 0.042 and 0.076 wt%. The lean deposit exhibited a rapid transformation to intermetallic phases on post-weld heat treatment, whilst the higher carbon deposit retained stable δ-ferrite after similar heat treatment. These results appear to be consistent with previously published transformation models for similar materials.

1. Introduction

The long-term creep ductilities of commercial manual metal arc duplex stainless steel weld metals are being studied by the power generation industry to enable better design-life predictions to be made for existing steam generating plant (piping and superheater tubes), and their projected use for nuclear power plant. The presence of δ-ferrite in these duplex weld metals, which is required to prevent hot cracking during welding, produces an inherent instability during service conditions through a complex series of phase reactions [1–4]. Previous studies on submerged arc weld metals have revealed that the δ-ferrite initially transforms to $M_{23}C_6$ carbides and austenite, followed by the transformation to intermetallic phases. These transformations are controlled by the localized enrichment of chromium and molybdenum within the δ-ferrite laths, and the proximity of the local composition to the ternary phase boundaries at the service temperatures [4].

The present work extends these studies with an investigation into the microstructural changes that occur with post-weld heat treatment and subsequent creep testing of two manual metal arc weld deposits. These had similar chromium, nickel and molybdenum contents, but different carbon levels and they had exhibited significantly different ductilities during creep testing at 600° C.

2. Experimental

The two lean AISI 316 type weld metals used in this study were deposited using commercial 4 mm manual metal arc rods with rutile coatings. The nominal compositions were 17% Cr, 8% Ni and 2% Mo with a controlled δ-ferrite content between 5 and 8%. The actual results obtained are given in Table I. The welding details and procedures are fully reported elsewhere [5].

Both of the welds were studied in the following conditions: (1) as-welded, (2) aged at 700° C for 15 h, (3) aged at 850° C for 8 h, (4) as in (2) or (3) and creep tested at 600° C. Suitable samples were taken from either the bulk deposit or machined creep specimens, for optical and electron optical examination in a manner similar to that used by Farrar and Thomas [3].

Microstructural and microcompositional analyses were carried out on a JEOL 100 CX scanning transmission electron microscope fitted with an energy dispersive analyser, EDX. Typical microcompositional analyses were carried out after accumulating 80 000–90 000 counts in 100 sec, giving a possible error of 0.25% in the calculated concentrations.

Samples were dissolved electrolytically at 2 V in 10% HCl–methanol to obtain the transformed phases. After suitable washing and centrifuging, these powders were analysed by X-ray diffraction, using Cr$K\alpha$ radiation, to determine the nature and amount of the δ-ferrite transformation products.

TABLE I Chemical analysis of weld metals (wt %)

Consumable type		C	Si	Mn	P	Si	Ni	Cr	Mo	Al	Ti	V	O*	N*	Schaeffler Cr equivalent	Schaeffler Ni equivalent	As-welded % δ-ferrite
Metrode RCF 17/8/2	BW 15	0.076	0.003	2.1	0.02	0.29	8.4	17.2	1.5	< 0.003	0.02	0.09	545	510	20.5	12.6	4.6
Metrode RCF 17/8/2L	BW 19	0.042	0.008	1.9	0.023	0.34	10.0	17.3	1.6	< 0.003	0.02	0.09	670	630	20.7	12.9	6.0

*Note oxygen and nitrogen analyses as p.p.m.

0022–2461/87 $03.00 + .12

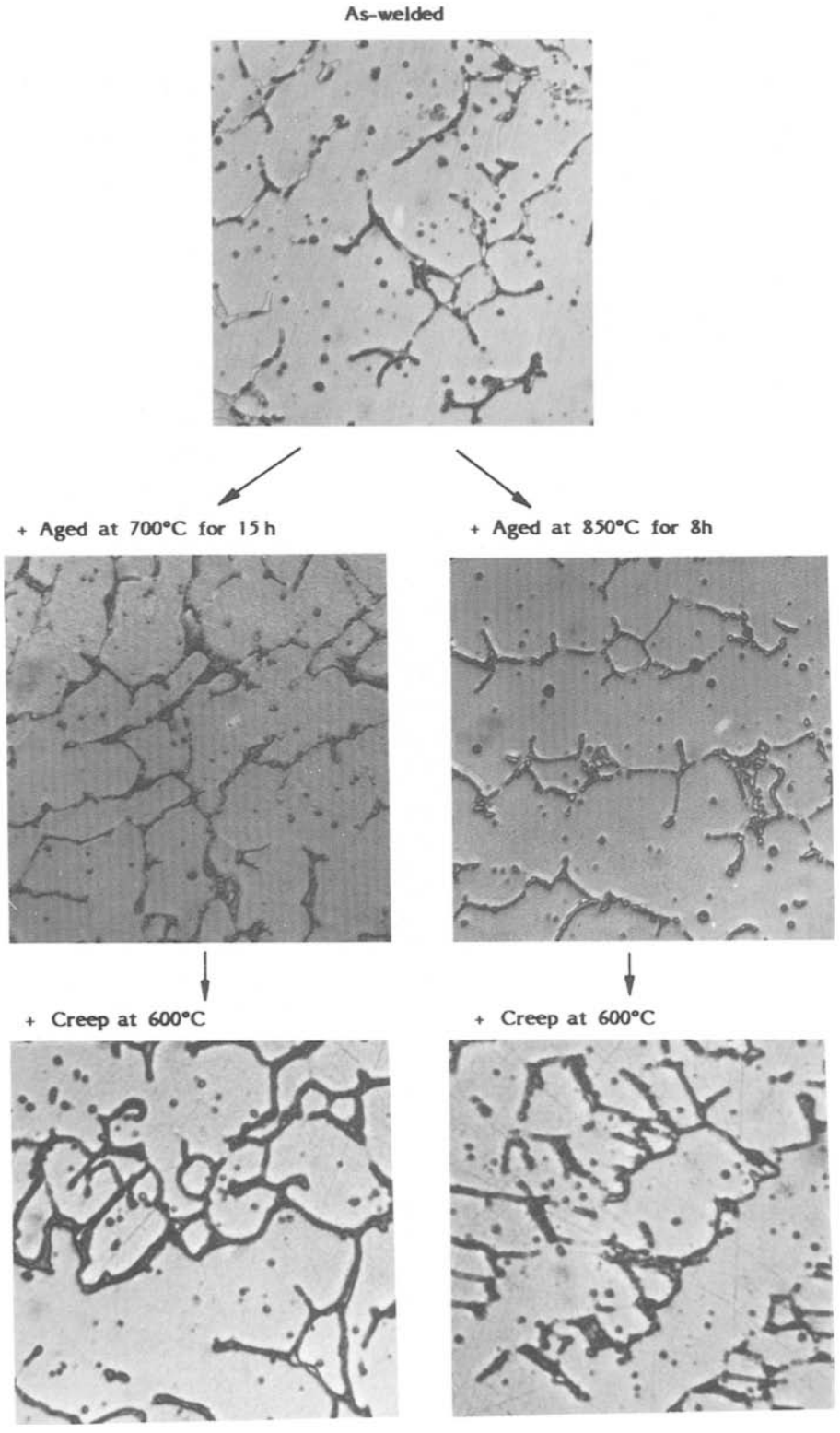

Figure 1 Weld metal BW 15 Etched in mixed acids, × 1250.

3. Results

3.1. Optical examination

Optical examination revealed quite distinctive differences between the two welds. In BW 15 there was evidence of some transformation of the δ-ferrite in the as-welded state, Fig. 1. Ageing at both 700 and 850° C appeared to enhance this precipitation and there was evidence of some spherodization occurring in the precipitates with the higher temperature treatment. Examination of the samples after creep testing at 600° C revealed evidence of further precipitation within the original δ-ferrite laths, Fig. 1.

In the case of the low carbon weld metal BW 19, optical examination revealed no evidence of transformation in the as-welded state, Fig. 2. The effect of ageing at 700° C was to produce obvious precipitation within the δ-ferrite, whilst ageing at 850° C produced ragged lath boundaries, which suggested that a major phase change had occurred, Fig. 2. This is similar to the effect observed by Thomas *et al.* [6]. Examination of the samples creep tested at 600° C following the 700° C heat treatment revealed clear evidence of further precipitation within the δ-ferrite. No material was creep tested following the 850° C heat treatment.

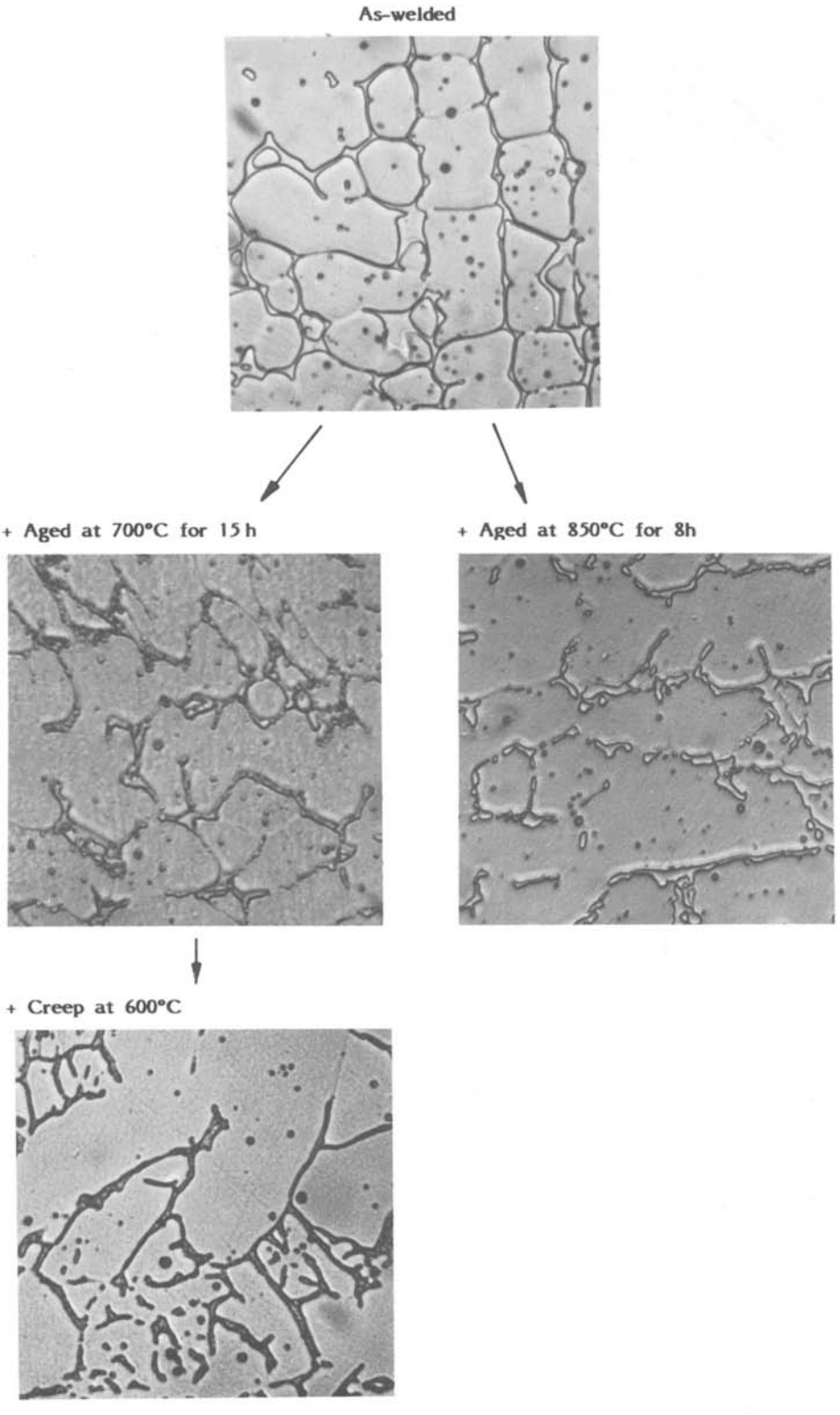

Figure 2 Weld metal BW 19. Etched in mixed acids, × 1250.

3.2. Hardness

An average of six hardness measurements on each of the samples revealed that both of the welds softened as a result of either of the initial heat treatments, Table II. In the case of weld BW 15, the as-welded value dropped from 206 VPN to 198 and 188 VPN, respectively, after ageing at 700 and 850° C. After creep testing at 600° C for some 19 000 h there was a substantial hardening of the specimen heat treated at 700° C, but little change in the other material.

TABLE II Vickers hardness numbers, VPN 10 kg

Weld metal	As-welded	Aged at 700° C	Aged at 850° C	Aged at 700° C plus creep at 600° C	Aged at 850° C plus creep at 600° C
BW 15	206	198	188	215	190
BW 19	186	183	175	180	n.d.

n.d. = not determined.

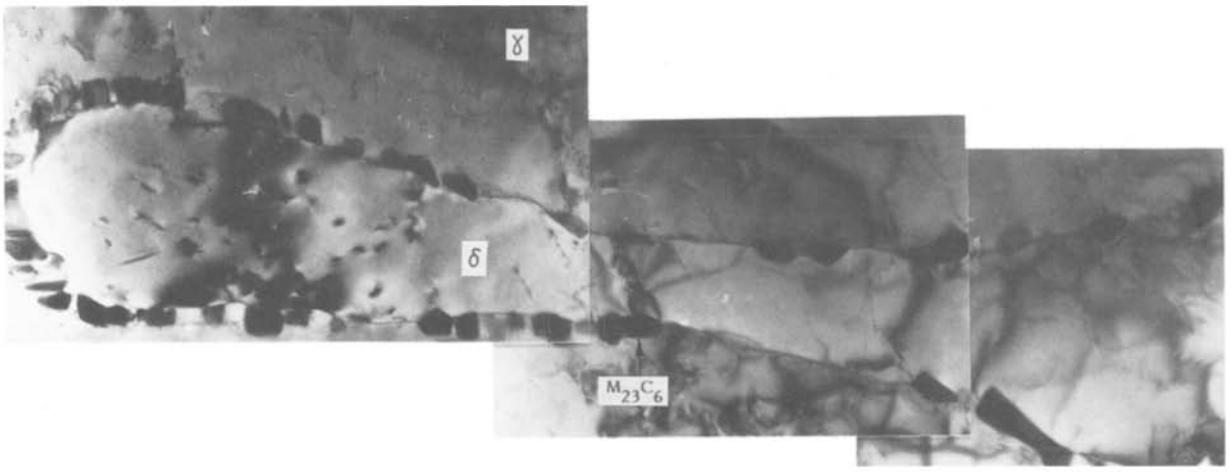

Figure 3 Transformation of δ-ferrite to carbides at the δ/γ boundaries in BW 15 material, as-welded, × 48 000.

Weld BW 19 was softer in both the as-welded and heat-treated states due to the lower carbon content. As with weld BW 15, the material dropped some 5 to 10 points of hardness depending on the heat treatment employed.

3.3. Delta ferrite phase transformation products

3.3.1. Weld metal BW 15

In the as-welded condition, electron diffraction confirmed that the δ-ferrite had transformed to $M_{23}C_6$ carbides at the δ/γ boundaries, Fig. 3. In some areas the transformation had occurred to a greater extent, Figs 4 and 5, and the loss of chromium and molybdenum from the original δ-ferrite had led to the transformation to austenite. This transformation is accompanied by a change in cell volume, and there is evidence of a high degree of strain appearing around the transforming ferrite in Fig. 4.

Close examination of the γ/γ boundaries revealed that there was little evidence of any precipitation occurring within the austenite matrix, Fig. 6.

After ageing at 700° C, some 50 to 75% of the δ-ferrite had transformed to a mixture of $M_{23}C_6$ carbides plus austenite, Fig. 7. In some of the laths there was still considerable evidence of strain bands being associated with this transformation, Fig. 8. The carbides had grown compared with the as-welded material, Fig. 9, and it was easy to confirm their structures by electron diffraction.

Close inspection of the austenite matrix revealed a limited amount of carbide precipitation at the γ/γ boundaries, Fig. 10, although it must be stressed that many of these boundaries were totally free from precipitation.

Ageing at 850° C allowed virtual completion of the δ-ferrite to carbide transformation, Fig. 11. This figure shows carbides decorating the original δ/γ boundaries, with virtually all the remaining lath volume having transformed to austenite. Electron diffraction indicated that the majority of the precipitates was $M_{23}C_6$ carbides plus a small amount of χ-phase. It was observed that the strain fields associated with the carbide precipitation were much smaller compared with those developed with the 700° C treatment, Fig. 12.

Examination of the austenite matrix and grain boundaries revealed a complete absence of any carbide precipitation.

Examination of the aged materials after some 19 000 h creep testing at 600° C, revealed that only small changes had occurred within the microstructure. The material heat treated at 700° C displayed a continuing transformation to $M_{23}C_6$ carbides, but there was still some 10 to 15% δ-ferrite remaining, Fig. 13. The large strain bands seen in the heat-treated material

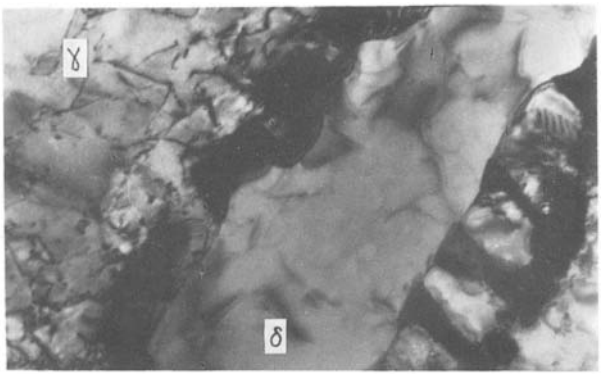

Figure 4 $M_{23}C_6$ carbides developing at the δ/γ boundaries of original δ-ferrite. These are associated with strain bands. BW 15, as-welded, × 69 930.

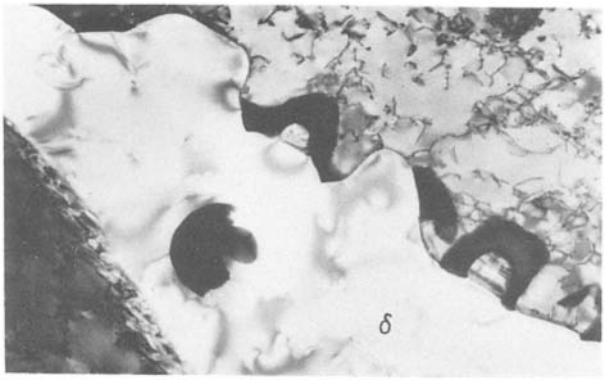

Figure 5 Transformation to $M_{23}C_6$ carbides and austenite at original δ/γ boundaries. BW 15, as-welded, × 26 640.

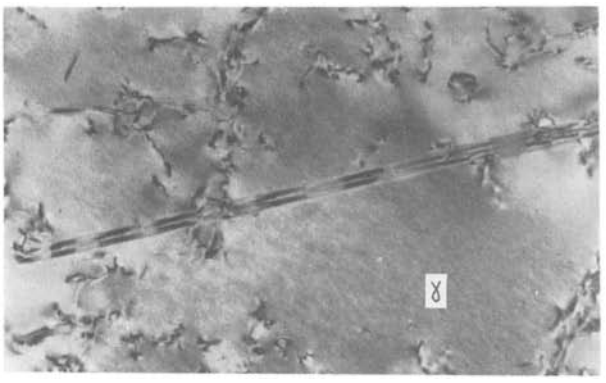

Figure 6 Absence of any precipitation within austenite matrix. BW 15, as-welded, × 69 930.

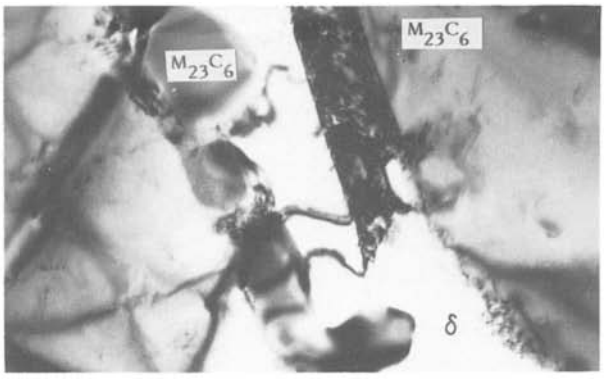

Figure 8 Strain associated with transformation of the δ-ferrite to $M_{23}C_6$ carbides and austenite. BW 15, aged at 700° C, × 53 280.

had almost disappeared, although there was still some evidence as seen in Fig.14. A small amount of precipitation was observed in the austenite matrix, Fig. 15, but it must be stressed that this was at a very low level. Electron diffraction evidence revealed that the majority of the precipitates was $M_{23}C_6$, with a small amount of possible M_6C appearing.

The presence of the greatly increased dislocation density seen in Fig. 13 is related to the high level of strain, 10.2%, produced during the creep testing of the specimen.

The material heat treated at 850° C displayed virtually a complete transformation to $M_{23}C_6$ carbides plus austenite, Fig. 16, with a significant spherodization of the carbides occurring, Fig. 17.

The general level of the dislocation density was higher than in the original heat-treated material, but again there was no systematic interaction of dislocations with any matrix precipitation, Fig. 18.

3.3.2. Weld metal BW 19

In the as-welded state, there were very clear δ-ferrite/austenite boundaries, which were completely free of any obvious precipitation, Figs 19 and 20, although they displayed faint fringe effects. This absence of precipitation is in marked contrast to the higher carbon level weld BW 15.

Examination of the austenite matrix and grain boundaries revealed no significant precipitation, Fig. 21.

After ageing at 700° C, electron diffraction confirmed that there was substantial transformation of the δ-ferrite to a mixture of $M_{23}C_6$ carbides + χ-phases, which accounted for some 70 to 75% of the original ferrite, Figs 22 and 23. Figure 24 reveals the intense strain patterns noted around many of the precipitates. In some areas of the microstructure the intermetallic phase had formed continuous films which could be detrimental to the mechanical properties.

A close examination of the austenite matrix revealed an absence of any significant precipitation, Fig. 24.

The heat treatment at 850° C produced a complete transformation to the intermetallic χ-phase plus a small amount of $M_{23}C_6$ carbides, Figs 25 and 26. There was also a very limited formation of σ-phase in this material. As with the material heat treated at 700° C there was a complete absence of any matrix precipitation, Figs 27 and 28.

Creep testing of the material aged at 700° C led to the complete transformation of the δ-ferrite to χ plus a small quantity of $M_{23}C_6$, Fig. 29, there was also an increase in the dislocation density.

3.4. Microcompositional segregation

As previous studies by Farrar and Thomas [3] had revealed that differences in the localized segregation of chromium, nickel and molybdenum could influence the nature and kinetics of the δ-ferrite transformation, the changes that occurred after the heat treatment were measured in the present work. The results, after using the correction factors reported by Farrar and Thomas [3], are given in Tables III and IV, for the two

Figure 7 Substantial development of $M_{23}C_6$ carbides at δ/γ boundaries after 15 h ageing at 700° C. BW 15, aged at 700° C, × 33 300.

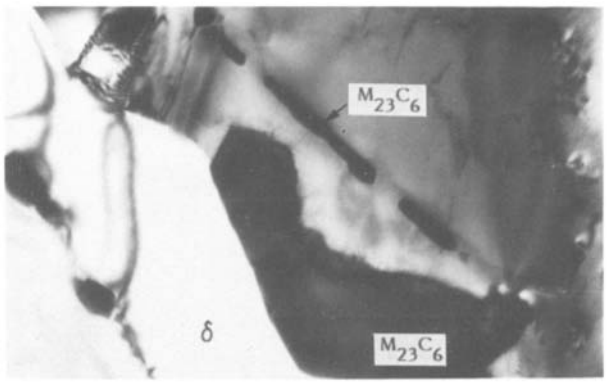

Figure 9 Massive $M_{23}C_6$ carbide development after ageing at 700° C for 15 h. Carbides also decorate original δ/γ boundaries. BW 15, aged at 700° C, × 53 280.

TABLE III Microsegregational analysis of phases in weld BW 15 wt %.

(a) δ-ferrite analysis

Condition	Cr	Ni	Mo	Mn	Schaeffler Cr equivalent	Schaeffler Ni equivalent
As-welded	21.6	4.2	0.7	0.8	22.5	4.7
+700° C for 15 h	20.2	4.0	0.6	0.6	21.2	4.3
+850° C for 8 h	21.2	3.8	1.4	0.8	23.0	4.2

(b) Precipitate phase analysis

Condition	Cr	Ni	Mo	Mn	Comments
As-welded	25.6	4.2	2.1	0.4	Only carbides present
+700° C for 15 h	27.9	4.2	2.7	0.3	Only carbides present
+850° C for 8 h	33.5	3.8	4.5	0.5	Carbides + very limited intermetallic formation

TABLE IV Microsegregational analysis of phases in weld BW 19 wt %.

(a) δ-ferrite analysis

Condition	Cr	Ni	Mo	Mn	Schaeffler Cr equivalent	Schaeffler Ni equivalent
As-welded	21.7	5.7	1.8	0.9	23.9	6.3
+700° C for 15 h	21.0	5.6	1.5	0.9	22.9	6.2
+850° C for 8 h	22.7	5.5	3.2	0.6	26.1	5.7

(b) Precipitate phase analysis

Condition	Cr	Ni	Mo	Mn	Comments
As-welded	–	–	–	–	No observable precipitates
+700° C for 15 h	25.5	5.3	2.1	0.6	Mixture of carbides + intermetallics
+850° C for 8 h	23.3	5.1	4.2	0.5	Mainly χ + σ phases + a few carbides

weld metals. It is interesting to notice that in both there is a tendency for the molybdenum content within the laths to rise with ageing at 850° C.

Tables III and IV also list the approximate Schaeffler chromium and nickel equivalents, together with the type of carbides and intermetallic phases observed.

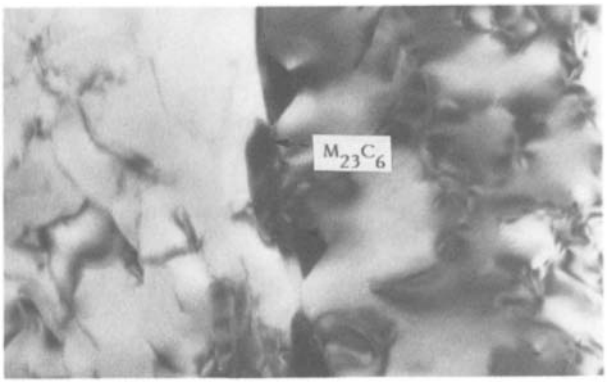

Figure 10 A few $M_{23}C_6$ carbides decorating a γ/γ boundary. BW 15, aged at 850° C, × 69 930.

3.5. X-ray diffraction

The results of the X-ray diffraction analyses are given in Table V. These results are in broad agreement with the electron optical observations and show that the weld material BW 15 contains mainly carbides in the as-welded and heat-treated at 700° C conditions, with only a limited intermetallic phase formation occurring with the 850° C ageing.

In the case of the weld BW 19, Table V shows that there is a significant amount of intermetallic phase formation occurring at both heat treatments, with χ being the dominant phase and σ only appearing in large quantities after the 850° C ageing.

The diffraction analyses also indicated the presence of very small quantities of niobium and titanium carbides. These carbides were not readily observable in the thin foil studies.

4. Discussion

4.1. Microsegregation effects and the role of carbon

Previous studies on submerged arc weld metals [3] suggested that the localized precipitation effects in the original δ-ferrite laths was controlled by the segregation of chromium and molybdenum to these laths during the welding operation; this segregation, coupled together with the proximity to the ternary phase boundaries and the diffusion of carbon from the

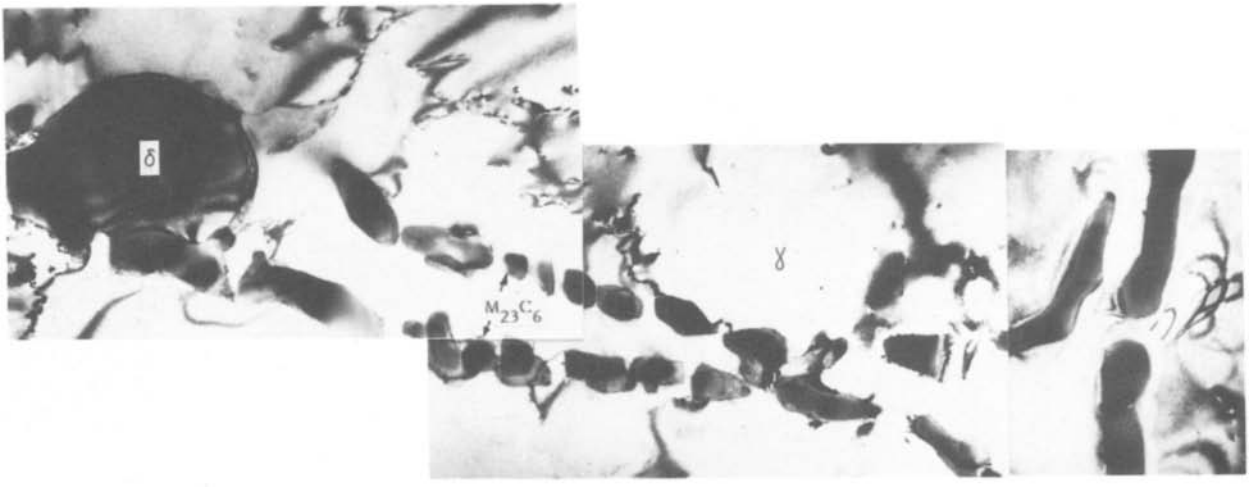

Figure 11 Virtually complete transformation of original δ-ferrite lath to carbides and austenite in BW 15 material aged at 850° C for 8 h, × 30 000.

TABLE V Type and amount of precipitation detected by bulk extraction X-ray analysis

(a) Weld BW 15

Condition	Phases present			Comments
	$M_{23}C_6$	Chi	Sigma	
As-welded	****	–	–	Small amount of TiCN + NbC present
Aged at 700° C for 15 h	*****	–	–	Small amount of NbC
Aged at 850° C for 8 h	****	**	*	small amount of NbC

(b) Weld BW 19

Condition	Phases present			Comments
	$M_{23}C_6$	Chi	Sigma	
As-welded	****	–	–	Small amount of NbC
Aged at 700° C for 15 h	**	****	*	Very small amount of NbC
Aged at 850° C for 8 h	*	****	**	–

* → ** → ***** Increasing proportions.

austenite at the operative temperature, then dominated the phase transformations.

The most significant difference between the two weld metals in this study is the level of carbon. Carbon will combine very rapidly with chromium and molybdenum in the δ-ferrite laths to form $M_{23}C_6$ carbides at the δ/γ boundaries. If the depletion of chromium and molybdenum by this reaction is sufficient then there is a strong possibility that the δ-ferrite will remain as a stable phase at the ageing temperature. As the diffusivity of carbon in austenite is very rapid [7], this reaction will occur during a multipass welding operation so that the as-welded material may already contain sufficient carbide precipitation to ensure stable δ-ferrite on subsequent ageing.

In the case of weld BW 15, this apparently is what has happened. There was sufficient carbon present in the weld to produce $M_{23}C_6$ carbides at an early stage of ageing, Fig. 3, and so stabilize the δ-ferrite, Fig. 12. Plotting the Schaeffler equivalents on to the

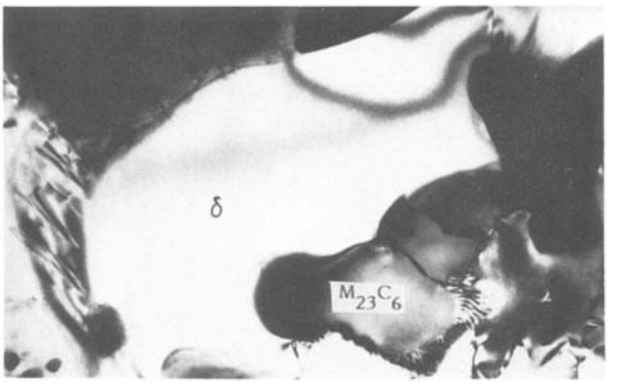

Figure 14 Transformation strains associated with $M_{23}C_6$ carbides following creep testing at 600° C. BW 15, aged at 700° C, × 69 930.

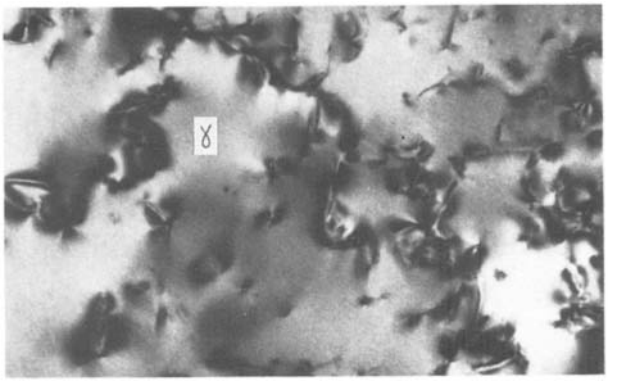

Figure 15 Matrix precipitation of carbides following creep testing at 600° C. BW 15, aged at 700° C, × 69 930.

Figure 12 Strain fields accompanying transformation to $M_{23}C_6$ carbides at δ/γ boundaries. BW 15, aged at 850° C, × 53 280.

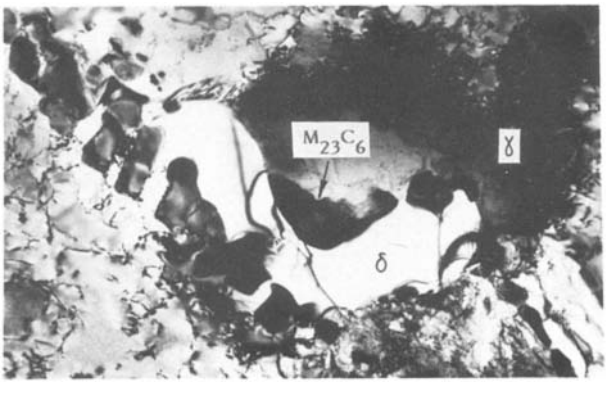

Figure 13 Development of $M_{23}C_6$ carbides following creep testing at 600° C. BW 15, aged at 700° C, × 21 312.

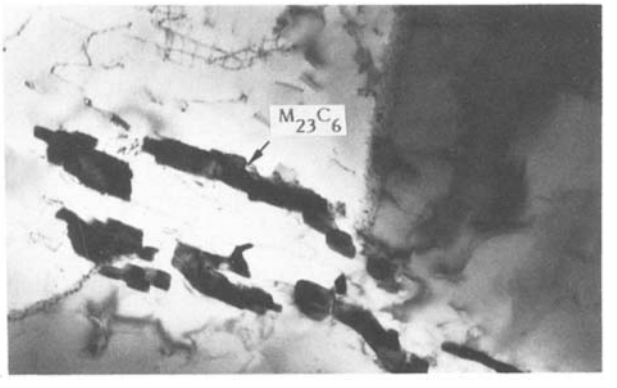

Figure 16 Complete transformation of original δ-ferrite lath to $M_{23}C_6$ carbides and austenite following creep testing at 600° C. BW 15, aged at 850° C, × 27 972.

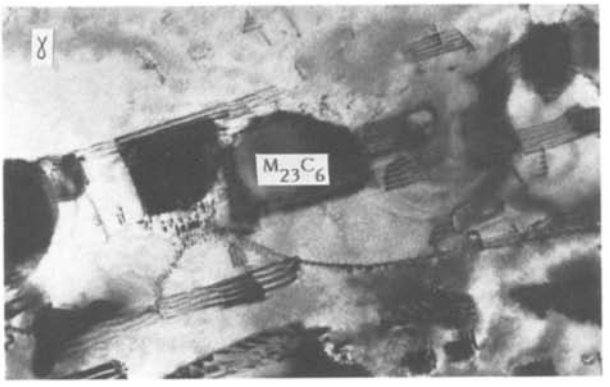

Figure 17 Partial spherodization of carbides following creep testing at 600° C. Evidence of strain fields and stacking faults within the austenite. BW 15, aged at 850° C, × 53 280.

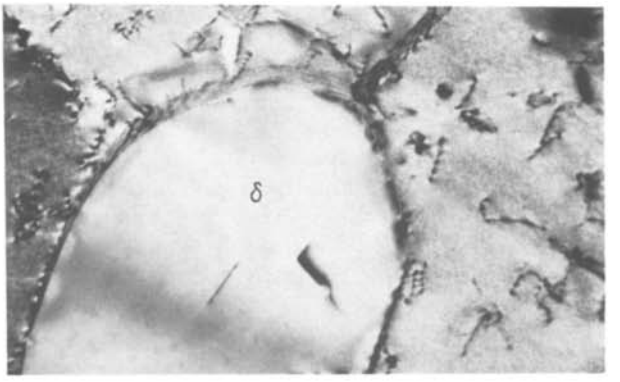

Figure 20 Slight fringe effects at the δ/γ boundary. BW 19, as-welded, × 53 280.

Figure 18 Very limited matrix precipitation in austenite after creep testing at 600° C. BW 15, aged at 850° C, × 69 930.

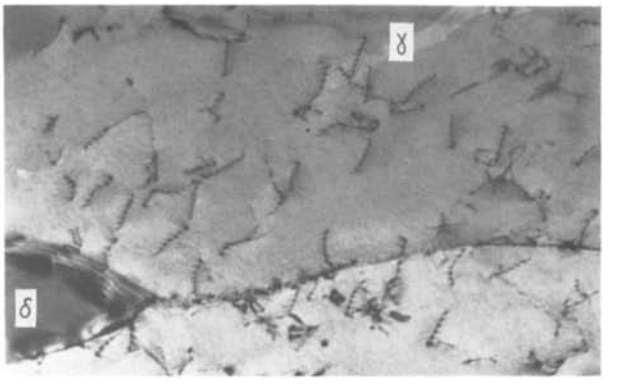

Figure 21 Absence of any precipitation at γ/γ boundaries in the as-welded material. BW 19, as-welded, × 53 280.

Fe–Cr–Ni ternary phase diagrams at 700 and 850° C, Figs 30 and 31, respectively, shows clearly that the compositions measured in the as-welded δ-ferrite laths lie within the $\delta + \gamma$ phases fields at both temperatures. The variations in the compositions measured, following ageing at 700 and 850° C, shown in Table III, do not alter this original picture. The small changes noted actually shift the δ-ferrite composition nearer to the appropriate phase boundary.

The composition of the precipitates observed at the δ/γ boundaries are consistent with this depletion model. The values measured at both the ageing temperatures revealed a significant increase in the chromium and molybdenum levels with a corresponding decrease in the nickel content.

It would seem that this precipitation of the $M_{23}C_6$ carbides, Fig. 9, is the dominant phase change and that the composition levels together with the lack of suitable nucleation sites within the δ-ferrite, limits any intermetallic phase formation.

Measurement of the segregation analyses in the weld BW 19 reveals a different state of affairs. The Schaeffler chromium and nickel equivalents when plotted on the Fe–Cr–Ni ternary diagrams, Figs 30 and 31, indicate that the δ-ferrite laths lie within the $\sigma + \gamma$ or $\delta + \gamma + \sigma$ fields at 700 and 850° C, respectively, This, coupled with the lack of carbide precipitation, encourages the δ-ferrite to transform to intermetallic phases with ageing, Figs 22 and 23.

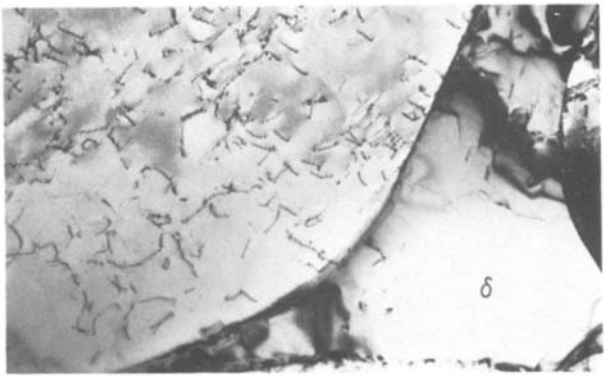

Figure 19 Absence of any carbide precipitation at the δ/γ boundaries in the as-welded condition, BW 19, as-welded, × 21 312.

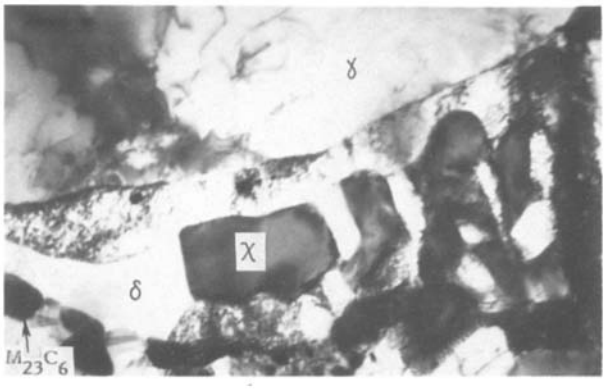

Figure 22 Complex transformation to a mixture of $M_{23}C_6$ carbides and intermetallic chi phase within original δ-ferrite lath. BW 19, aged at 700° C, × 35 298.

Figure 23 Very complex transformation to mixture of carbides and intermetallic phases, accompanied by intense strain bands. BW 19, aged at 700° C, × 53 280.

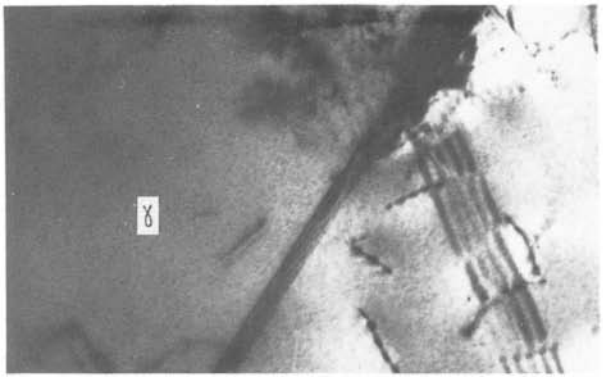

Figure 24 Limited precipitation at γ/γ boundaries. BW 19, aged at 700° C, × 106 560.

It is suggested that the critical element which controls this intermetallic precipitation is molybdenum. Whereas in weld BW 15, the molybdenum is removed by $M_{23}C_6$ carbide precipitation during the early stages of ageing, the lower level of carbon in BW 19 means that the molybdenum is still available within the δ-ferrite laths and intermetallic phase formation will be encouraged. This intermetallic phase reaction takes place quite quickly, so that ageing at 700° C for 15 h produces a significant amount of χ-phase, Fig. 26.

A similar model was used for submerged arc weld metals aged at 700° C [3]. This work suggested that the incorporation of molybdenum into the grain-boundary carbides [8] could eventually produce some

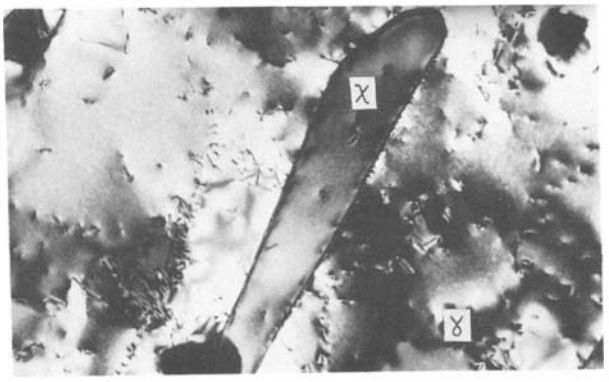

Figure 25 Complete transformation of original δ-ferrite lath to intermetallic χ-phase. BW 19, aged at 850° C, × 17 316.

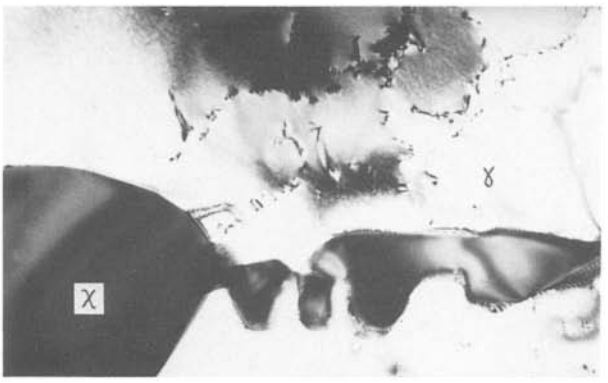

Figure 26 Partial sperodisation of transformed intermetallic χ-phase following ageing at 850° C. BW 19, aged at 850° C, × 35 298.

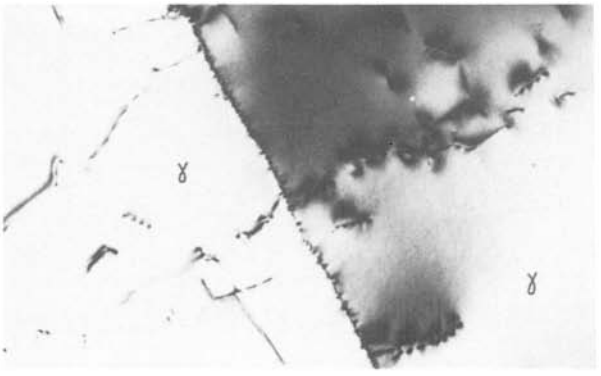

Figure 27 Absence of any precipitation on γ/γ boundaries. BW 19, aged at 850° C, × 69 930.

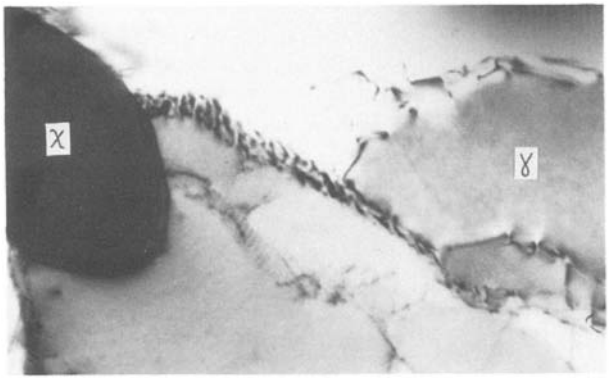

Figure 28 Absence of any precipitation in austenite matrix. BW 19, aged at 850° C, × 53 280.

Figure 29 Complete transformation of original δ-ferrite laths to intermetallic χ-phase following creep testing at 600° C. BW 19, aged at 700° C, × 13 320.

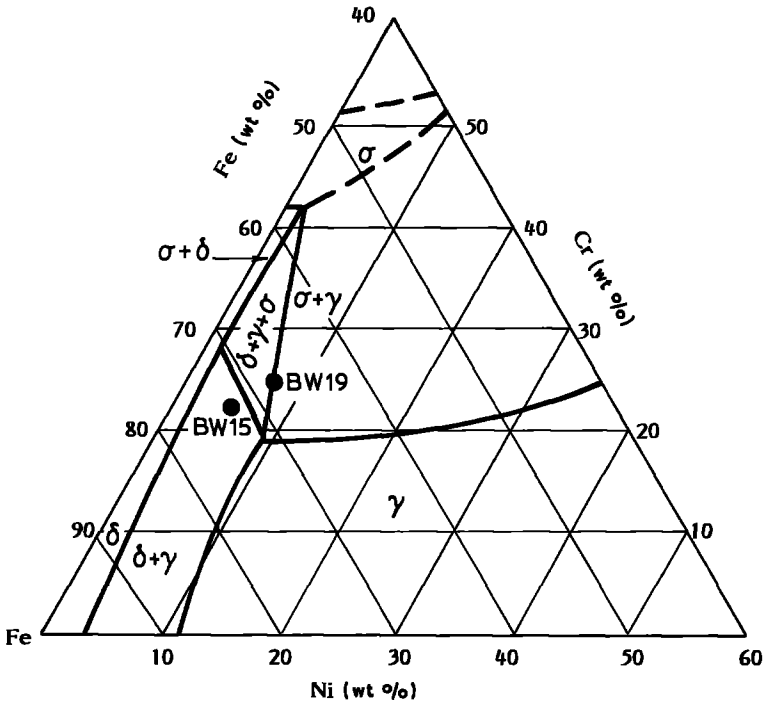

Figure 30 700° C isotherm of the Cr–Fe–Ni system showing the composition of the as-welded δ-ferrite.

transformation of the $M_{23}C_6$ carbides to M_6C following the 700° C heat treatment.

The further removal of molybdenum will enhance the δ-ferrite stability and allow localized transformation to austenite. Fig. 15 shows carbides outlining an original δ-ferrite lath, but with the interior completely transformed to austenite, with a localized composition similar to the bulk chemical analysis.

4.2. Transformation kinetics

The transformation data obtained from the electron diffraction studies on aged material from weld BW 15 can be compared with earlier work which has been recently summarized in the form of a time–temperature–precipitation (TTP) diagram for 17/8/2 weld metals [5]. The current results from weld metal BW 15 have been used to improve the accuracy of this diagram in the temperature range 700 to 850° C, Fig. 32. It can be seen that the initial heat treatments would have produced only $M_{23}C_6$ carbides at 700° C and only a very limited amount of intermetallic phases at 850° C. It was not possible to include the results from weld BW 19, which due to its much lower carbon content, will have different phase transformation kinetics.

4.3. Implications for creep properties

Initial comparisons between the microstructural changes and the creep properties [9] of these alloys reveals significant differences between the two initial heat treatments. The creep results for both weld metals aged at 700° C suggest a lower initial creep ductility and longer secondary stage compared with the material aged at 850° C. Typical creep results for

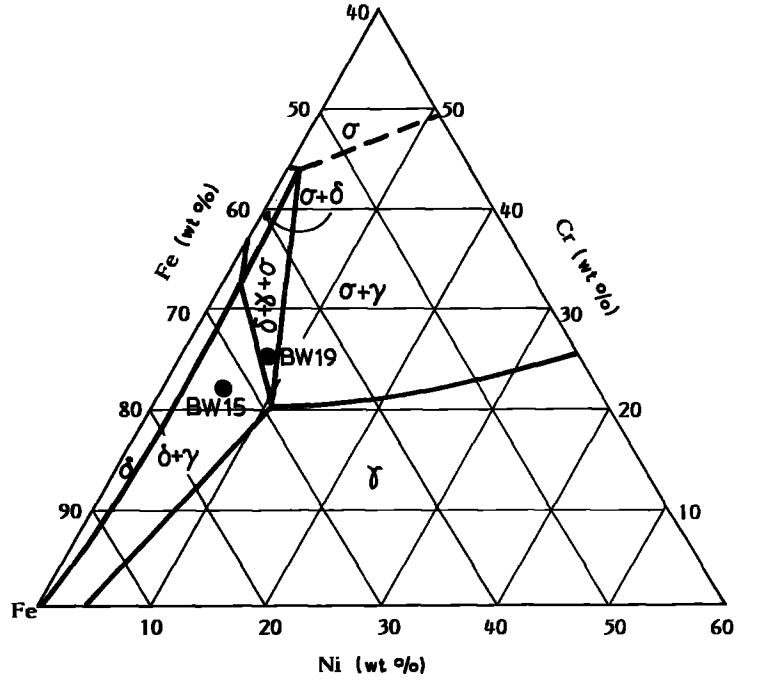

Figure 31 850° C isotherm of the Cr–Fe–Ni system showing the composition of the as-welded δ-ferrite.

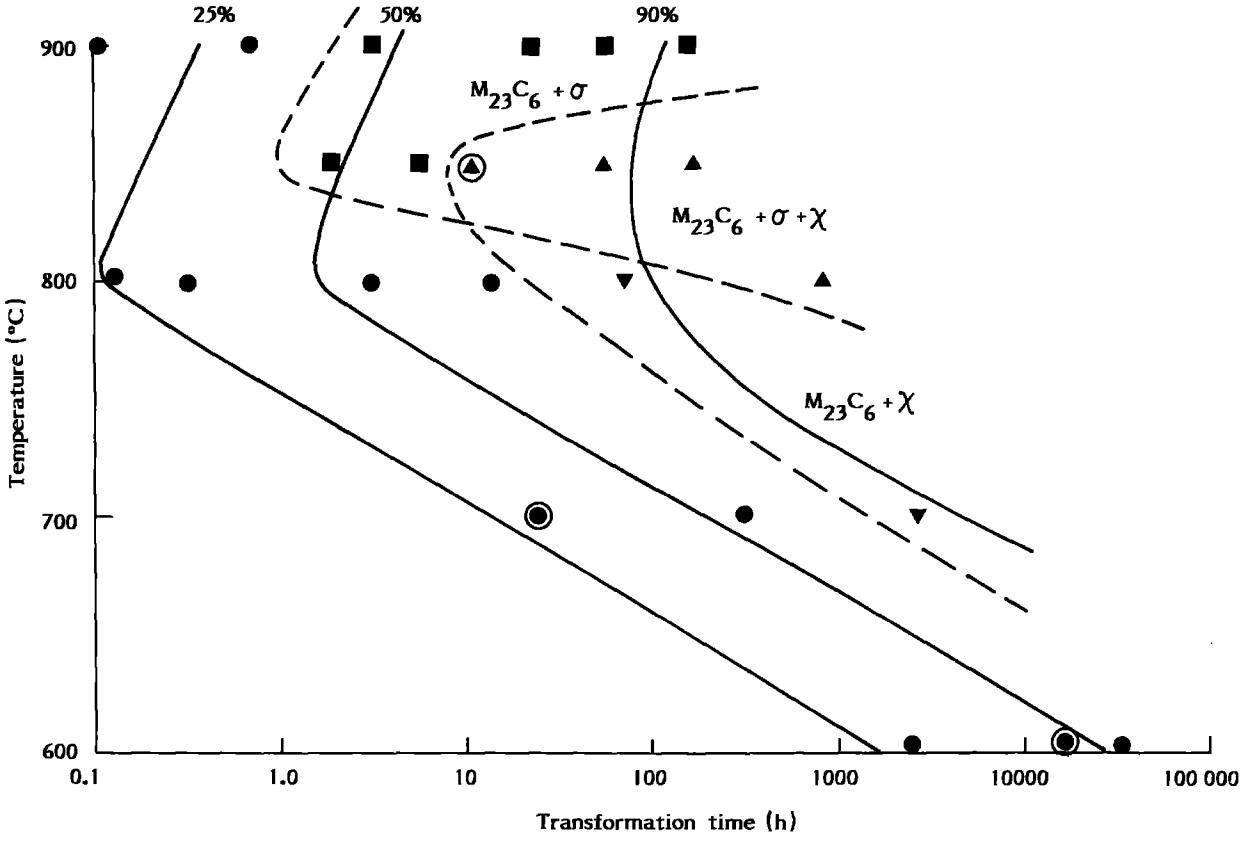

Figure 32 Transformation kinetics of 17/8/2 MMA weld metals, after Farrar *et al.* [5]. Phases identified: (●) $M_{23}C_6$, (■) $M_{23}C_6 + \sigma$, (▼) $M_{23}C_6 + \chi$, (▲) $M_{23}C_6 + \sigma + \chi$. (——) % ferrite transformed. ◉, ◬, present work.

material tested at 600° C and at a stress of 170 MPa gave secondary lives of ~16 000 h and ~8000 h, respectively, for the 700 and 850° C heat treatments. A similar difference was seen in the total strain to fracture which decreased from 11.6% to 7.2% for the same initial heat treatments.

High-temperature creep is known to involve both slip within the matrix and grain-boundary sliding, so that changes at the grain boundaries will have an effect on the creep behaviour as well as mechanisms which involve dislocation recovery.

5. Conclusions

1. Heat treatment at 700° C produces only carbides in the normal carbon level weld BW 15, but a rapid transformation to χ-phase in the low carbon weld metal BW 19.

2. Heat treatment at 850° C produces a small amount of intermetallic χ-phase coupled with a significant spherodization of the carbides in weld metal BW 15. In the case of weld metal BW 19 only intermetallic χ-and σ-phases are formed.

3. Carbon is dominant in determining the stability of the δ-ferrite. This ensures that in the creep regime, the δ-ferrite remains stable or slowly converts to austenite.

4. The rate of transformation and the nature of the transformation products appears to depend on the proximity of the initial segregation values in the δ-ferrite to the Fe–Cr–Ni phase field boundaries.

5. The phase rections observed in these MMA weld metals follow similar trends to submerged arc weld metals examined in earlier work. It suggests that suitable adjustments to the carbon and molybdenum levels coupled with appropriate heat treatments can produce improved welding consumables for use in the temperature range 550 to 700° C.

Acknowledgements

This work was carried out at the Marchwood Engineering Laboratories, where the author is a Visiting Research Officer, and the paper is published with the permission of the Central Electricity Generating Board. The author also wishes to acknowledge the continued interest of Dr J. Myers, CEGB, Marchwood, and Dr R. G. Thomas, CEGB, Barnwood.

References

1. S. R. KEOWN and R. G. THOMAS, *Met. Sci.* **15** (1981) 386.
2. R. G. THOMAS and S. R. KEOWN, "Mechanical behaviour and nuclear applications of stainless steel at elevated temperatures", Varese Conference, May 1981 (Metal Society, London, 1982) Book 280, p. 30.
3. R. A. FARRAR and R. G. THOMAS, *J. Mater. Sci.* **18** (1983) 3461.
4. R. A. FARRAR, *ibid.* **20** (1985) 4215.
5. R. A. FARRAR, C. HUELIN and R. G. THOMAS, *ibid.* **20** (1985) 2828.
6. R. G. THOMAS, R. D. NICHOLSON and R. A. FARRAR, *Met. Tech.* **11** (1983) 373.
7. T. M. DEVINE, *J. Met. Trans. A* **11A** (1980) 791.
8. B. WEISS and R. STICKLER, *Met. Trans.* **3** (1972) 851.
9. J. B. MYERS, CEGB Report TPRD/M/1509/R85 (1985).

Received 4 March
and accepted 22 May 1986